Indian Journal of Chemistry
Vol. 64, November 2025, pp. 1038-1048
DOI: 10.56042/ijc.v64i11.18497

Computational investigation of the antioxidant activity of sesamol and its *ortho*-amino derivatives in polar and nonpolar environments: Quantum chemical, molecular docking and drug likeness studies

Fatiha Djazia Larbaoui, Sidi Mohamed Mekelleche* & Khadidja Bellifa

Laboratory of Applied Thermodynamics and Molecular Modelling, Department of Chemistry, Faculty of Science, University of Tlemcen, PB 119, Tlemcen, 13000, Algeria

E-mail: sidi_mekelleche@yahoo.fr, sidimohamed.mekelleche@univ-tlemcen.dz

Received 3 April 2025; accepted (revised) 30 October 2025

The natural sesamol, present in the seeds and oil of sesame, has attracted considerable interest for its powerful antioxidant properties. Its ability to neutralise free radicals and to inhibit lipid peroxidation highlight its potential as a therapeutic agent to reduce the oxidative stress. This explains the beneficial effects of sesamol as an effective protector against the damaging effects of reactive oxygen species (ROS). The antioxidant activity of sesamol and its *ortho*- mono- and di-substituted amino (R= NH_2, NHMe and NHCN) derivatives has been investigated at the SMD//M06-2X/6-311+G(d,p) computational level. The calculations have been performed in the gas phase and in non-polar (toluene) and polar (ethanol and water) solvents. The main mechanisms, namely, HAT, SPLET and SET-PT have been thoroughly investigated and analysed. The obtained results put in evidence that HAT and SPLET are the thermodynamically favoured mechanisms in non-polar and polar media respectively, while SET-PT is found to be a disfavoured mechanism in all media. The obtained results also show that di-substitution with strong electron-donating groups in the *ortho*- position leads to significant increase in their antioxidant activity compared to the reference molecule (sesamol). The antioxidant activity of the sesamol derivatives has also been evaluated by molecular docking to explore the possible interactions of each compound with the Xanthine Oxidase (XO) enzyme which is responsible for ROS generation and the obtained results show that these derivatives exhibit high binding affinities to the active site of the XO enzyme. Finally, the studied compounds satisfy both Lipinski and Veber drug likeness properties and could be considered as good radical scavengers.

Keywords: Sesamol, Oxidative stress, Antioxidant activity, DFT calculations, Molecular docking, Drug likeness

Free radicals have a potential role in the regulation of many cellular biochemical processes, in particular reactive oxygen species (ROS), which are implicated in neurodegeneration[1]. However, their excessive production disrupts the balance of antioxidant homeostasis, leading to a state of oxidative stress[2]. This imbalance between free radicals and antioxidant defence systems in physiological processes damages proteins, lipids and DNA[3], contributing to neurodegenerative disorders such as Alzheimer's and Parkinson's diseases[2,4], as well as other conditions such as cardiovascular disease[5], cancer and early aging[6]. This justifies the beneficial effects of endogenous and exogenous antioxidants as effective protectors against the harmful effects of ROS. Given the growing number of reports of complications associated with oxidative stress, compounds with antioxidant activities are attracting keen interest as potential candidates for preventing disease and slowing the aging process. This is the background to the study of sesamol's effect on oxidative stress.

Natural sesamol, also known as lignan, found in the seeds and oil of sesame[7], a tropical oilseed plant ubiquitous throughout the world, has long been valued and employed as a traditional health supplement. It is a phenol derivative which possesses several biological activities and therapeutic properties, making it a promising candidate for the treatment of many ROS-induced diseases, whose protective functions have been widely reported, including anti-inflammatory[8–10], anti-mutation[11,12], anti-cancer[13,14], anti-aging[15,16], neuroprotective[17–19] and lipid peroxidation inhibitory effects[16,20,21] due to its antioxidant properties[10,12,21–30].

Numerous experimental[7,10,18,21,31–33] and theoretical[12,22–24,34] studies reported in the literature have highlighted the potential role of sesamol as an antioxidant. For instance, Palheta *et al*.[22] investigated

by molecular modelling at the B3LYP/6-31+G(d,p) and B3LYP/6-311++G(2d,2p) levels of theory, the antioxidant activity of sesamol through a molecular modification strategy by alkylation, inspired by natural and synthetic antioxidants. All the proposed derivatives[22] were compared with related classical antioxidants such as Trolox, t-butylhydroxytoluene (BHT) and t-butyl hydroxy anisole (BHA) and their results show that alkyl substitutions at the *ortho* position to the phenolic moiety were more effective than all other positions. In another work, Palheta *et al.*[12] found that the antioxidant activity of sesamol is comparable to Trolox. Castro-Gonzalez *et al.*[23] performed a computational design of sesamol derivatives, using a computer assisted protocol, by inclusion of different functional groups in *ortho* and *meta* positions of sesamol and found that the antioxidant activity in enhanced by electron donating groups. Najafi *et al.*[24] carried out a theoretical study of several *ortho* and *meta* mono-substituted sesamol derivatives by B3LYP/6-31G(d,p) method in gas phase and in water. Their results show that electron-donating substituents in the *ortho* position increase remarkably the antioxidant capacity. This says that *ortho* mono-substitution is better than *meta* mono-substitution of sesamol. Moreover, Najafi *et al.*[24] also found that amino groups (NH_2, NHMe, NMe_2) are better than the other electron donating groups (*t*-Bu, Et, Me, Ph, $CH=CH_2$, OH, OMe). However, the influence of di-substitution of sesamol by amino electron-donating groups in the two *ortho* positions remains to be explored.

Our aim in the present work is to carry out a computational study of the antioxidant activity of sesamol **SES** and its *ortho* mono-substituted **A1-A3**, **B1-B3** and di-substituted **C1-C3** amino derivatives (Fig. 1). More specifically, we analyse and compare the effect of mono-substitution in each of the two *ortho* positions, as well as the effect of di-substitution by amino electron-donating groups (NH_2, NHMe, NHCN). This enables us to identify the position offering the best antioxidant power and radical scavenging capacity. This present study aims to highlight the thermodynamically most favourable mechanism (HAT/SPLET/ SET-PT) in non-polar and polar environments and to predict the most promising sesamol derivatives by the calculation of the suitable thermochemical descriptors. We are also analysing the binding affinity of sesamol and its potential amino derivatives to the active site of the enzyme xanthine oxidase (XO). The drug-likeness properties of these derivatives are also being evaluated on the basis of Lipinski and Veber rules.

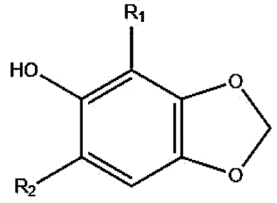

Sesamol
SES: R_1=R_2=H
Mono-substituted sesamol derivatives
A1: R_1=NH_2, R_2= H B1: R_1=H, R_2= NH_2
A2: R_1=NHMe, R_2= H B2: R_1=H, R_2= NHMe
A3: R_1=NHCN, R_2= H B3: R_1=H, R_2= NHCN
Di-substituted sesamol derivatives
C1: R_1= R_2=NH_2
C2: R_1= R_2= NHMe
C3: R_1= R_2= NHCN

Fig. 1 — Chemical structures of Sesamol and its designed derivatives

Computational Details

The optimisation of the geometries of the studied compounds was performed with the Gaussian 09 package[35] using the density functional theory (DFT) at the M06-2X[36] level of theory and the standard 6-311+G(d,p) basis set. The vibrational frequencies of the studied compounds were calculated at the same level of theory in order to confirm that all the stationary points correspond to real minima on the potential energy surface. The M06-2X functional has been chosen because of its high performance in thermochemistry and for its accuracy in reactions involving free radicals[36,37]. It was also successfully used in the estimation of bond dissociation energies and kinetics[37–40]. This study was carried out in the gas phase (ε=1) and in a variety of solvents, namely toluene (ε = 2.37), ethanol (ε = 24.85) and water (ε= 78.35) in order to simulate the lipid (non-polar) and polar (extracellular and blood serum) environments[41]. The implicit universal solvation model based on solute electron density (SMD) was used because it is suitable for both charged and uncharged solutes in a wide range of solvents and liquid media[42]. It has also been shown to be appropriate for geometry optimisation and vibrational calculations in solution[43]. The three well-known mechanisms of antioxidant activity[24,44–50] have been explored and analysed, namely hydrogen atom transfer (HAT), sequential proton loss followed by electron transfer (SPLET) and single electron transfer followed by proton transfer (SET-PT). The overview of the three mechanisms is shown in Scheme 1, also detailed in equations (1), (2a), (2b), (3a) and (3b) given below. The thermodynamic parameters associated with the studied antioxidant mechanisms were computed using the provided

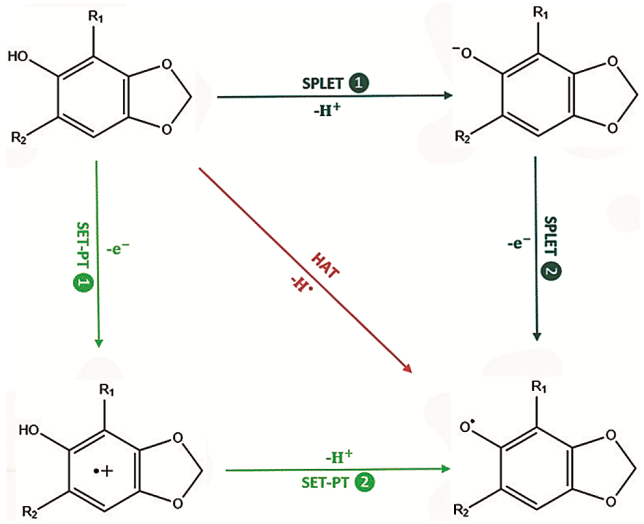

Scheme 1 — Schematic representation of the three mechanisms HAT, SPLET and SET-PT of the antioxidant activity

equations at a temperature of 298.15 K and pressure of 1 atm.

- HAT (Hydrogen Atom Transfer)

$$\text{BDE (Bond Dissociation Enthalpy)} = H(Ar - O^{\bullet}) + H(H^{\bullet}) - H(Ar - OH) \quad \text{... (1)}$$

- SPLET (Sequential Proton Loss-Electron Transfer)

(Step 1):

$$\text{PA (Proton Affinity)} = H(Ar - O^{-}) + H(H^{+}) - H(Ar - OH) \quad \text{... (2a)}$$

(Step 2):

$$\text{ETE (Electron Transfer Enthalpy)} = H(Ar - O^{\bullet}) + H(e^{-}) - H(Ar - O^{-}) \quad \text{... (2b)}$$

- SET-PT (Single Electron Transfer-Proton Transfer)

(Step 1):

$$\text{IP(Ionisation potential)} = H(Ar - OH^{\bullet+}) + H(e^{-}) - H(Ar - OH) \quad \text{... (3a)}$$

(Step 2):

$$\text{PDE (Proton Dissociation Enthalpy)} = H(Ar - O^{\bullet}) + H(H^{+}) - H(Ar - OH^{\bullet+}) \quad \text{... (3b)}$$

The favoured mechanism is determined by the lower values of BDE, PA and IP. In other words, the lowest value of the descriptor of the first step of the mechanism (HAT/SPLET/SET-PT) implying that the enthalpy of the first step is determining[51,52]. The ranking of the antioxidant activity of the studied compounds in different environments was evaluated by the thermodynamic values of BDE_{min} for HAT, $(PA+ETE)_{min}$ for SPLET and $(IP+PDE)_{min}$ for SET-PT[4,40].

Results and Discussion

Geometry optimisation

The equilibrium geometries of the studied compounds, namely, sesamol **SES** and its derivatives **A1-A3**, **B1-B3** and **C1-C3** were optimised at the M06-2X/6-311+G(d,p) computational level. It should be noted that the optimised geometry of sesamol was obtained using the X-ray structure, downloaded from the CCSD database[53], and used as an initial guess. The perfect atom-by-atom superimposition between the X-ray and optimised structures (Fig. 2), together with the very low value of the root-mean-square deviation (RMSD=5.93×10^{-7} Å), show that the used level of theory is suitable for geometry optimisation of sesamol derivatives.

Standard enthalpies of hydrogen atom, proton, and electron in vacuum and in polar and non-polar solvents

It's important to note that the accurate assessment of the thermodynamic descriptors responsible for antioxidant activity requires the knowledge of the standard enthalpies of the hydrogen atom ($H^{\bullet}$), the proton (H^{+}), and the electron (e^{-}), both in vacuum (gas phase) and in different solvents. The estimated values of the standard enthalpies of these three species in vacuum and in the considered solvents were obtained from the literature[4,54–56] and are presented in Table 1. The standard enthalpy of a solvated species X was calculated using the following equation:

$$H°(X_{solvated}) = H°(X)_{vacuum} + \Delta H°_{solvation}(X) \quad \text{... (3)}$$

where X denotes either a hydrogen atom ($H^{\bullet}$), a proton (H^{+}), or an electron (e^{-}).

Theoretical study of the antioxidant activity in polar and non-polar environments

Antioxidant activity in non-polar environments

Table 2 and Table 3 show the calculated thermochemical descriptors for sesamol and its derivatives in the gas phase and in toluene, respectively.

From the results obtained in Table 2 and Table 3, HAT was found to be the dominant mechanism in gas phase and in toluene. This is justified by the low BDE values compared to PA values (first step of SPLET) and IP values (first step of SET-PT). This statement is

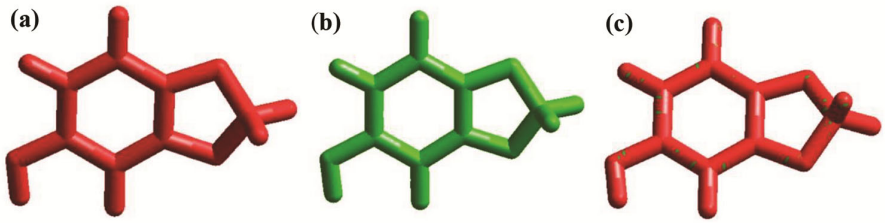

Fig. 2 — (a) X-Ray structure (red), (b) gas phase optimised structure (green) and (c) atom by atom superimposition of the X-ray and optimised structures of sesamol (RMSD=5.93×10^{-7} Å)

Table 1 — Standard enthalpies (in kJ.mol^{-1}) of hydrogen atom, proton, and electron in vacuum and in the studied solvents.

Species	Enthalpy H°	Solvation Enthalpy $\Delta H°_{solv}$ (kJ.mol^{-1})		
	Vacuum	Solvents		
	Gas phase	Toluene	Water	Ethanol
Hydrogen atom ($H^{\bullet}$)	–1306.553[a]	5.1[d]	–4[d]	3.7[d]
Proton (H^{+})	6.197[b]	–911.7[c]	–1055.7[c]	–1064[c]
Electron (e^{-})	3.146[c]	–15.2[c]	–77.5[c]	–56.3[c]

[a] from the Ref. 4
[b] from the Ref. 56
[c] from the Ref. 54
[d] from the Ref. 55

Table 2 — Calculated thermodynamic parameters (in kJ.mol^{-1}) of sesamol and its designed derivatives in gas phase

	HAT		SPLET			SET-PT	
Ligand	BDE	PA	ETE	PA+ETE	IP	PDE	IP+PDE
SES	337.80	1444.38	209.32	1653.70	739.33	914.37	1653.70
A1	311.40	1440.54	186.76	1627.30	727.69	899.61	1627.30
A2	304.20	1435.15	184.95	1620.10	718.50	901.60	1620.10
A3	317.63	1375.72	257.81	1633.53	775.58	857.95	1633.53
B1	288.63	1434.18	170.35	1604.53	660.52	944.01	1604.53
B2	280.51	1433.04	163.37	1596.41	640.32	956.09	1596.41
B3	302.42	1370.75	247.56	1618.32	731.76	886.56	1618.32
C1	266.74	1424.20	158.43	1582.64	641.75	940.89	1582.64
C2	265.56	1431.49	149.96	1581.45	625.59	955.86	1581.45
C3	279.69	1305.22	290.37	1595.59	755.80	839.79	1595.59

Table 3 — Calculated thermodynamic parameters (in kJ.mol^{-1}) of sesamol and its designed derivatives in toluene

	HAT		SPLET			SET-PT	
Ligand	BDE	PA	ETE	PA+ETE	IP	PDE	IP+PDE
SES	338.90	421.01	301.78	722.80	604.74	118.06	722.80
A1	314.24	419.47	278.66	698.13	597.10	101.03	698.13
A2	306.90	415.99	274.81	690.79	591.68	99.11	690.79
A3	322.32	370.99	335.23	706.22	632.88	73.34	706.22
B1	289.99	415.88	258.00	673.88	531.48	142.40	673.88
B2	281.47	415.47	249.89	665.36	515.77	149.59	665.36
B3	307.34	368.94	322.30	691.24	596.44	94.80	691.24
C1	271.57	408.98	246.49	655.46	517.47	137.99	655.46
C2	268.74	416.44	236.20	652.63	505.81	146.83	652.63
C3	287.92	320.23	351.59	671.82	619.42	52.40	671.82

verified for sesamol **SES** and all its derivatives **A1-A3**, **B1-B3** and **C1-C3**. Il turns out that all the designed derivatives are better than the reference molecule **SES** (BDE=338.90 kJ.mol^{-1}). Moreover, for mono-substituted derivatives, **B1-B3** are better than **A1-A3**. On the other hand, the di-substituted derivatives **C1-C3** are better than mono-substituted derivatives **B1-B3**. Consequently, the following increased sequence order of the antioxidant activity is obtained:

SES < **B3** < **B1**< **B2** < **C3** < **C1**< **C2** (in gas phase and in toluene)

It is great of interest to note that presence of the strong electron donating NHMe group (in **B2** and **C2**) decreases remarkably the BDE value compared to other amino groups (*i.e*. NH_2 and NHCN). We notice the presence of strong hydrogen bonding between the oxygen atom of the final Ar-O• radical and the hydrogen atom of the amino group of the studied compounds and this intramolecular stabilising interaction is absent *in tertio* amino groups (for instance NMe_2).

Antioxidant activity in polar environments

The calculated thermochemical descriptors in ethanol and water are given in Table 4 and Table 5 respectively.

Based on the results given in Table 4 and Table 5, the PA values are lower than BDE and IP values. Accordingly, SPLET is the thermodynamically most favoured mechanism in polar solvents, namely ethanol and water. In addition, PA values decrease with increasing solvent polarity, indicating that the deprotonation process is more favoured in strong polar solvents. We note that the SET-PT mechanism is disfavoured in all solvents.

On the other hand, the comparison of (PA+ETE) values of the studied compounds leads to conclude that the $(PA+ETE)_{min}$ values of C**1-C3** derivatives are lower than those of B**1-B3** and **A1-A3** derivatives and the parent molecule **SES**, indicating that the *ortho*

Table 4 — Calculated thermodynamic parameters (in kJ.mol^{-1}) of sesamol and its designed derivatives in ethanol

	HAT	SPLET			SET-PT		
Ligand	BDE	PA	ETE	PA+ETE	IP	PDE	IP+PDE
SES	339.36	166.99	364.27	531.26	480.85	50.41	531.26
A1	309.01	158.12	342.78	500.90	476.44	24.47	500.90
A2	311.43	165.24	338.09	503.33	482.87	20.46	503.33
A3	329.03	145.84	375.09	520.92	503.66	17.27	520.92
B1	290.47	166.84	315.53	482.37	416.43	65.94	482.37
B2	282.65	165.94	308.60	474.54	404.39	70.16	474.54
B3	314.34	145.75	360.49	506.24	468.27	37.97	506.24
C1	279.88	163.84	307.93	471.77	417.98	53.80	471.77
C2	271.27	164.89	298.28	463.17	415.78	47.39	463.17
C3	301.35	120.39	372.86	493.25	485.52	7.73	493.25

Table 5 — Calculated thermodynamic parameters (in kJ.mol^{-1}) of sesamol and its designed derivatives in water

	HAT	SPLET			SET-PT		
Ligand	BDE	PA	ETE	PA+ETE	IP	PDE	IP+PDE
SES	330.46	160.11	357.05	517.16	457.05	60.11	517.16
A1	300.67	151.24	336.13	487.37	453.54	33.83	487.37
A2	294.78	148.61	332.87	481.48	440.42	41.06	481.48
A3	320.82	141.67	365.85	507.52	479.68	27.84	507.52
B1	281.23	159.97	307.96	467.93	393.54	74.39	467.93
B2	274.12	158.77	302.05	460.82	382.75	78.07	460.82
B3	305.66	141.56	350.80	492.36	444.08	48.28	492.36
C1	271.80	156.81	301.68	458.49	396.12	62.37	458.49
C2	262.97	155.62	294.04	449.67	391.57	58.10	449.67
C3	294.17	129.76	351.11	480.87	461.46	19.41	480.87

disubstituted amino derivatives of sesamol are the better antioxidants of the studied series. The comparison of $(PA+ETE)_{min}$ of **C1-C3** gives the following order of the antioxidant capacity: **C3** < **C1** < **C2** (in ethanol and water). We note that the methyl group (in NHMe of **C2**) increases the antioxidant activity while the cyano group (in NHCN of **C3**) decreases it.

Spin density distribution

Reactive oxygen species (ROS) are considered harmful and potentially dangerous free radicals due to their high spin density (close to unity) on the oxygen atom which gives them a high degree of reactivity. In order to illustrate the stability of the final Ar-O$^{\bullet}$ radicals (Scheme 1), the atomic spin densities were calculated. The spin density distributions corresponding to the radical forms of sesamol **SES** and its derivatives **A1-A3**, **B1-B3** and **C1-C3** in gas phase are given in Fig. 3.

The results show that the spin density values of the oxygen atom of all the studied radicals, in gas phase, are between 0.25 and 0.33, meaning that the spin density is not concentrated on the oxygen atom of Ar-O$^{\bullet}$ radicals but delocalised over the entire molecule, indicating that the great stability of Ar-O$^{\bullet}$ radicals is due to spin density delocalisation. We can conclude that sesamol and its amino derivatives are good candidates for the antioxidant activity since they generate stable radicals.

Molecular Docking

The sesamol **SES** and its designed derivatives (**A1-A3**, **B1-B3** and **C1-C3**) have demonstrated a promising capacity to neutralize free radicals. To better assess whether these compounds might have inhibitory potential against enzymes known to generate reactive oxygen species (ROS)[57], a molecular docking study was carried out. One of these enzymes is xanthine oxidase (XO), which is being

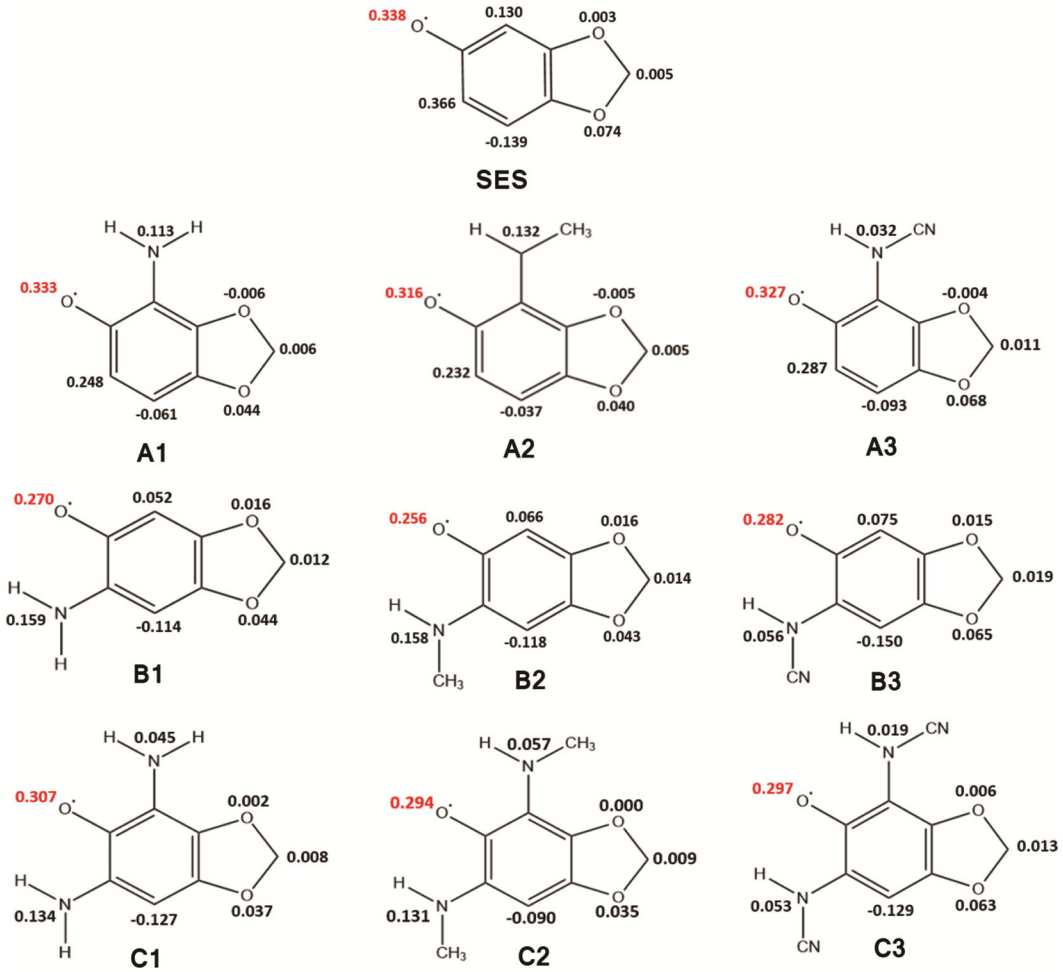

Fig. 3 — The spin density distributions in Ar-O• radicals of sesamol and its designed derivatives in gas phase

studied in particular due to its implication in the pathophysiology of various human diseases[58]. XO catalyses the oxidation of xanthine and hypoxanthine into uric acid[59]. This process is accompanied by the release of reactive oxygen species[60], which can induce oxidative stress and contribute to the development of gout[61]. The inhibition of this enzyme contributes to attenuating oxidative stress, thereby offering protection against the development of several diseases. In light of this, the studied compounds have been docked onto the active site of XO. The crystal structure of bovine xanthine oxidase co-crystallised with quercetin (PDB ID: **3NVY**, resolution 2 Å)[62] was obtained from the PDB database[63]. Protein/ligand preparation, receptor grid generation and docking were performed with Auto-Dock tools 1.5.7 (Ref. 64) by adding missing hydrogen atoms, fusing non-polar hydrogen atoms and assigning Kollman charges for protein preparation, as for ligand 3D structures, they were prepared and optimised using Gaussian software then, with ADT Gasteiger partial charges were added and rotating bonds were defined. Grid maps of dimensions 40 - 40 - 40 Å were prepared with a spacing of 0.375 Å using Auto-Grid. Other Auto-Dock parameters were set to their default values. Molecular docking used the Lamarckian genetic algorithm (LGA). The figures were created using BIOVIA Discovery Studio[65].

By examining Table 6, where the binding affinity and amino acids are reported, it turns out that the studied ligands are able to interact with the active site of xanthine oxidase and to exhibit a strong binding affinity towards XO. Indeed, the calculated binding free energies for **SES**, **A1**, **A2**, **A3**, **B1**, **B2**, **B3**, **C1**, **C2** and **C3** derivatives are -5.91, -6.49, -6.68, -7.07, -6.63, -6.5, -7.02, -6.92, -6.96 and -7.66 kcal.mol^{-1} respectively.

Fig. 4 shows that the studied compounds are surrounded by several amino acid residues identified as catalytic. The studied ligands establish hydrogen bonds with ARG880, GLU802, THR1010, GLU1261, SER876 and ALA1079, among which GLU802, GLU1261 and ARG880 play an essential role in the catalytic function of the XO enzyme[62,66]. Ligand

Table 6 — Results of molecular docking of sesamol and its designed derivatives with the XO enzyme

Ligand	Binding free energy (kcal.mol^{-1})	Ki (μM)	Amino acids involved
SES	–5.91	46.57	ARG880, THR1010, SER876, GLU802, VAL1011, LEU873, ALA1079, LEU1014, PHE914, PHE1009
A1	–6.49	17.39	ARG880, THR1010, SER876, GLU802, GLU879, VAL1011, LEU1014, LEU873, ALA1079, PHE914, PHE1009
A2	–6.68	12.74	ARG880, GLU802, SER876, Val1010, SER1008, ALA910, THR1010, PHE1009, PHE914, LEU1014, LEU873, PRO1076, ALA1078, ALA1079
A3	–7.07	6.52	GLU802, ALA1079, THR1010, PHE1009, PHE914, Val1011, LEU1014, ALA1078, ARG880, SER1008, SER876, LEU873, PRO1076
B1	–6.63	13.74	ARG880, GLU802, ALA910, PRO1076, LEU873, LEU1014, SER876, Val1011, THR1010, PHE914, PHE1009, ALA1078, ALA1079
B2	–6.5	17.12	ARG880, THR1010, GLU802, GLU1261, SER876, SER1008, PHE914, PHE1009, Val1011, LEU1014, ALA1078, ALA1079
B3	–7.02	7.17	ARG880, THR1010, SER876, GLU802, GLU1261, SER1008, VAL1011, LEU1014, ALA1078, ALA1079, PHE914, PHE1009
C1	–6.92	8.41	THR1010, GLU802, GLU1261, ARG880, PHE1009, PHE1005, GLY913, ALA910, PRO1076, LEU873, LEU1014, SER876, Val1011, ALA1078, ALA1079
C2	–6.96	7.89	THR1010, GLU802, ARG880, SER876, PRO1076, LEU648, LEU873, SER1008, LEU1014, ALA1079, Val1011, PHE1009, PHE914
C3	–7.66	2.43	ARG880, GLU802, SER876, THR1010, VAL1011, LEU873, LEU1014, PRO1076, ALA910, GLU1261, PHE914, PHE1009, ALA1078, ALA1079

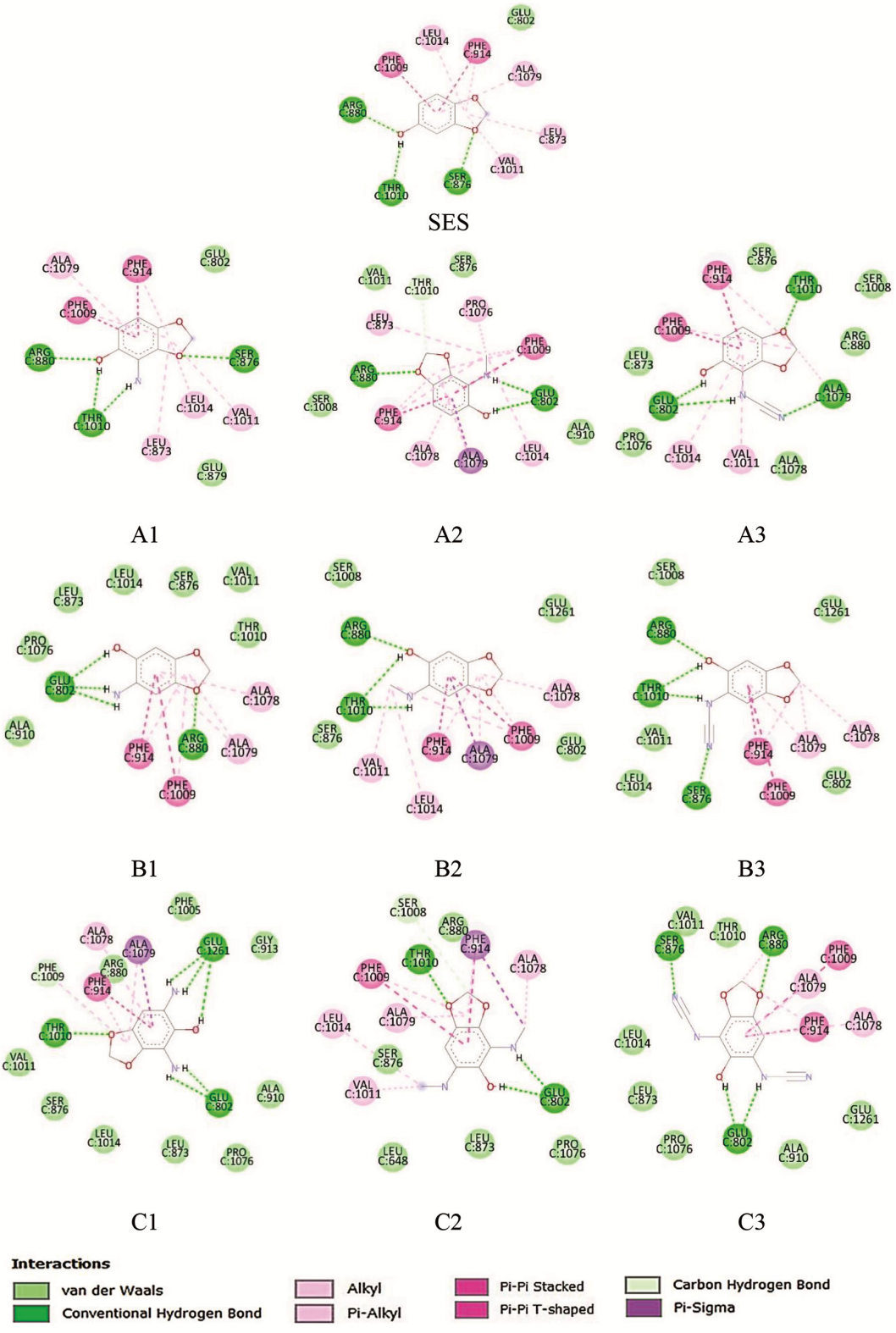

Fig. 4 — 2D representation of complexes formed between ligands SES, A1-A3, B1-B3, C1-C3 and XO enzyme by molecular docking

Table 7 — Drug-likeness parameters for sesamol SES and its designed derivatives A1-A3, B1-B3 and C1-C3

Compd	Smiles	Lipinski rules				Veber rules	
		MW (amu) ≤500	Log P ≤5	HBD ≤5	HBA ≤10	TPSA (Å^2) ≤140	NRB ≤ 10
SES	O1c2ccc(O)cc2OC1	138.122	1.121	1	3	38.69	0
A1	O1c2ccc(O)c(c2OC1)N	153.137	0.703	2	4	64.71	0
B1	O1c2cc(c(O)cc2OC1)N						
A2	O1c2ccc(O)c(c2OC1)NC	167.164	1.163	2	4	50.72	1
B2	O1c2cc(c(O)cc2OC1)NC						
A3	O1c2ccc(O)c(c2OC1)NC#N	178.147	1.014	2	5	74.51	1
B3	O1c2cc(c(O)cc2OC1)NC#N						
C1	O1c2cc(c(O)c(c2OC1)N)N	168.152	0.285	3	5	90.73	0
C2	O1c2cc(c(O)c(c2OC1)NC)NC	196.206	1.204	3	5	62.75	2
C3	O1C2=CC(C(O)C(=C2OC1)NC#N)NC#N	220.188	–1.029	3	7	110.33	2

stabilisation in the active site is enhanced by the presence of other residues, such as LEU1014, LEU648, LEU873, PHE914, PHE1009 and VAL1011.

These findings lead to the conclusion that the designed derivatives act as potential inhibitors of the XO enzyme and interact favourably with certain amino acid residues which are important for the XO catalytic function, confirming their antioxidant capacity.

Drug likeness properties of sesamol and its derivatives

The parameters of drug likeness are criteria used to assess whether a chemical substance has the potential to become an effective and safe medicament or food supplement. These parameters are typically based on rules or physicochemical descriptors that have been associated with the success of drugs on the market. The Lipinski and Veber rules are two well-known examples of drug likeness criteria. The Lipinski rules are based on four criteria: molecular weight less than 500 Daltons, LogP (octanol/water partition coefficient) less than 5, the number of hydrogen bond donors (HBD) less than or equal to 5, and the number of hydrogen bond acceptors (HBA) less than or equal to 10. If a molecule satisfies these rules, it is considered to have a good chance of success as a drug. The Veber rules focus on the polarity and flexibility of the molecule. They state that the number of rotatable bonds (NRB) in the molecule should not exceed 10, and the total polar surface area (PSA) should not exceed 140 Å^2. These criteria aim to ensure good intestinal absorption and cellular permeability. In this study, we evaluated the drug likeness parameters for sesamol **SES** and its designed derivatives using the ADMETlab server[67]. Based on the parameters, given in Table 7, the studied molecules (**SES**, **A1-A3**, **B1-B3** and **C1-C3**) verify all these criteria. Consequently, the studied systems can be considered as promising candidates for food supplement development.

Conclusion

The present work highlights the crucial role of *ortho* di-substitution by strong electron-donating groups, showing increased efficiency compared to mono-substitution. The obtained results reveal that the introduction of amino electron-donating substituents in the two *ortho* positions relative to the phenolic group leads to a notable stabilisation of free radicals and a significant enhancement of the antioxidant activity of sesamol derivatives compared to the reference system. The SET-PT mechanism is disfavoured in all environments, while the HAT mechanism is favoured in non-polar solvent and the SPLET is preferred in polar media. The di-substitution of sesamol with NH_2, NHMe, NHCN amino groups demonstrated potent antioxidant capacity, even better than sesamol, particularly NHMe, which proved to be the most effective substituent, due to the presence of the hydrogen bond in radical species, exhibiting the lowest BDE value in lipidic medium and the lowest value of the sum (PA+ETE) in polar medium. According to docking scores, the studied compounds show a strong binding affinity with the active site of the XO enzyme. These results suggest that the studied compounds could act as potential inhibitors of xanthine oxidase, paving the way for the development of new treatments for reducing the oxidative stress. The assessment of the drug likeness properties of sesamol and its derivatives

indicates that all parameters fall within the expected ranges and comply with Lipinski's and Veber rules, this suggests that the compounds under investigation possess favourable oral bioavailability and satisfactory drug likeness properties. In summary, it is clear that the NHMe *ortho* disubstituted sesamol predicted to be the most effective radical scavenger among the other derivatives studied in all environments and could represent a promising compound for scavenging free radicals.

Data availability

All relevant data and findings of this study are included within the article. No additional external data was used.

Author Contributions

Sidi Mohamed Mekelleche conceptualised the project. The computational analysis, including quantum chemical calculations, molecular docking and prediction of drug likeness properties, were performed by Fatiha Djazia Larbaoui. The manuscript was written by Fatiha Djazia Larbaoui, Sidi Mohamed Mekelleche and Khadidja Bellifa. All authors read and approved the final manuscript for publication.

Conflict of Interest

The authors declare no conflicts of interest.

Funding information

This research project was funded by the Algerian Ministry of Higher Education and Scientific Research (PRFU Project Number B00L01UN130120220006).

Acknowledgments

The authors are grateful to the University of Tlemcen for high-performance computing cluster facilities.

References

1 Emerit J & Edeas M, Bricaire F, *Biomed Pharm,* 58 (2004) 39.
2 Ruankham W, Suwanjang W, Wongchitrat P, Prachayasittikul V, Prachayasittikul S & Phopin K, *Nut Neurosci*, 24 (2021) 90.
3 Amić A, Marković Z, Marković J M D, Jeremić S, Lučić B & Amić D, *Comp Bio Chem,* 65 (2016) 45.
4 Mansouri H & Mekelleche S M, *J Theor Comp Chem*, 19 (2020) 2050032.
5 Sachidanandam K, Fagan S C & Ergul A, *Cardiovasc, Drug Rev,* 23 (2006) 115.
6 Hajam Y A, Rani R, Ganie S Y, Sheikh T A, Javaid D, Qadri S S, Pramodh S, Alsulimani A, Alkhanani M F, Harakeh S, Hussain A, Haque S & Reshi M S, *Cells,* 11 (2022) 552.
7 Majdalawieh A F & Mansour Z R, *Eur J Pharm*, 855 (2019) 75.
8 Yashaswini P S, Kurrey N K & Singh S A, *Food Chem,* 228 (2017) 330.
9 Huang J, Sun Q, Song G, Qi S, Chen J, Zhang P, Geng T, Lin Q & Duan Y, *LWT*, 123 (2020) 109077.
10 Guo Y, Fan J, Qu L, Bao C, Zhang Q, Dai H & Yang R, *Ind Crops Prod*, 141 (2019) 111762.
11 Chen W Y, Chen FY, Lee A S, Ting K H, Chang CM, Hsu J F, Lee W S, Sheu J R, Chen C H & Shen M Y, *J Nat Prod*, 78 (2015) 225.
12 Palheta I C & Borges R S, *Chem Data Coll*, 11 (2017) 77.
13 Liu Z, Xiang Q, Du L, Song G, Wang Y & Liu X, *Food Chem*, 141(2013) 289.
14 Bosebabu B, Cheruku S P, Chamallamudi M R, Nampoothiri M, Shenoy R R, Nandakumar K, Parihar V K & Kumar N, *Mini-Rev Med Chem*, 20 (2020) 988.
15 Morawska K, Festinger N, Chwatko G, Głowacki R, Ciesielski W & Smarzewska S, *Food Chem*, 309 (2020) 125789.
16 Nayak P G, Paul P, Bansal P, Kutty N G & Pai K S R, *J Pharm Pharm*, 65 (2013) 1083.
17 Hou R C W, Chen Y S, Chen C H, Chen Y H & Jeng K C G, *J Biomed Sci*, 13 (2006) 89.
18 Yaswanatha K N L, Bharathi K K N, Mudgal J, Vasantha Raju S G & Manohara R S A, *Results Chem,* 3 (2021) 100095.
19 Javed H, Meeran M F N, Jha N K, Ashraf G M & Ojha S, *Curr Top Med Chem,* 24 (2024) 797.
20 Shah A, Lobo R, Krishnadas N & Surubhotla R, *Indian J Pharm Educ Res,* 53 (2019) 2s.
21 Zhou S, Zou H, Huang G & Chen G, *Bioorg Med Chem Lett*, 31 (2021) 127716.
22 Palheta I, Ferreira L, Vale J, Silva O, Herculano A, Oliveira K, Neto A M J C, Campos J, Santos C & Borges R, *Molecules,* 25 (2020) 3300.
23 Castro-González L M, Alvarez-Idaboy J R & Galano A, *ACS Omega,* 5 (2020) 9566.
24 Najafi M, Najafi M & Najafi H, *Can J Chem*, 90 (2012) 915.
25 Nair A B, Dalal P, Kadian V, Kumar S, Garg M, Rao R, Almuqbil R M, Alnaim A S, Aldhubiab B & Alqattan F, *Plants*, 12 (2023) 1168.
26 Joshi R, Kumar M S, Satyamoorthy K, Unnikrisnan M K & Mukherjee T, *J Agric Food Chem,* 53 (2005) 2696.
27 Castro-González L M, Galano A & Alvarez-Idaboy J R, *New J Chem,* 45 (2021) 11960.
28 Guo Y, Wang Y, Xu B & Li Y, *Nutr Neurosci,* 1 (2025)..
29 Huang L, Yang J, Liang Z, Liang R, Luo H, Sun Z, Han D & Niu L, *Biosensors,* 13 (2023) 859.
30 Nair A B, Dalal P, Kadian V, Kumar S, Kapoor A, Garg M, Rao R, Aldhubiab B, Sreeharsha N, Almuqbil R M, Attimarad M, Elsewedy H S & Shinu P, *Nanomaterials,* 12 (2022) 4211.
31 Xie Y, Liu J, Shi Y, Wang B, Wang X, Wang W, Sun M, Xu X, Jiang H, Guo M, He Y, Ren C & Cheng L, *Bioorg Med Chem Lett,* 44 (2021) 128121.
32 Rashed K, *Plantae Sci,* 5 (2022) 8.
33 Buravlev EV, Shevchenko O G & Suponitsky K Yu, *Chem Biodivers*, 18 (2021) e2100221.
34 Hong Y, Li J-B, Siddiqui M K, Nazeer W & Najafi M, *Russ J Phys Chem A*, 92 (2018) 2757.

35 Frisch M J, Trucks G W, Schlegel H B, Scuseria G E, Robb M A, Cheeseman J R, Scalmani G, Barone V, Mennucci B, Petersson G A, Nakatsuji H, Caricato M Li X, Hratchian H P, Izmaylov A F, Bloino J, Zheng G, Sonnenberg J L, Hada M, Ehara M, Toyota K, Fukuda R, Hasegawa J, Ishida M, Nakajima T, Honda Y, Kitao O, Nakai H, Vreven T, Montgomery J A, Peralta J E, Ogliaro F, Bearpark M, Heyd J J, Brothers E, Kudin K N, Staroverov V N, Kobayashi R, Normand J, Raghavachari K, Rendell A, Burant J, Iyengar S S, Tomasi J, Cossi M, Rega N, Millam J M, Klene M, Knox J E, Cross J B, Bakken V, Adamo C, Jaramillo J, Gomperts R, Stratmann R E, Yazyev O, Austin A J, Cammi R, Pomelli C, Ochterski J W, Martin R L, Morokuma K, Zakrzewski V G, Voth G, Salvador P, Dannenberg J J, Dapprich S, Daniels A, Farkas Foresman J B, Ortiz J V, Cioslowski & Fox D J, *Gaussian 09*, (Revision C.01, Gaussian, Inc., Wallingford), 2009.

36 Zhao Y & Truhlar D G, *Theor Chem Acc,* 120 (2008) 215.

37 Mansouri H & Mekelleche S M, *J Comp Biophys Chem,* 20 (2021) 829.

38 Galano A & Alvarez-Idaboy J R, *J Comp Chem,* 35 (2014) 2019.

39 Vo Q V, Tam N M, Hieu L T, Van Bay M, Thong N M, Le Huyen T, Hoa N T & Mechler A, *RSC Adv,* 10 (2020) 14937.

40 Bellifa K & Mekelleche S M, *J Comp Biophys Chem,* 21 (2022) 167.

41 Galano A, Francisco-Márquez M & Alvarez-Idaboy J R, *Phys Chem Chem Phys,* 13 (2011), (23) 11199

42 Marenich A V, Cramer C J & Truhlar D G, *J Phys Chem B,* 113 (2009) 6378.

43 Ribeiro R F, Marenich A V, Cramer C J & Truhlar D G, *J Phys Chem B,* 115 (2011) 14556.

44 Škorňa P, Rimarčík J, Poliak P, Lukeš V & Klein E, *Comp Theor Chem,* 1077 (2016) 32.

45 El-Hadj Saïd A, Mekelleche S M & Ardjani T E A, *Can J Chem,* 96 (2018) 453.

46 Najafi M, Najafi M & Najafi H, *Comp Theor Chem,* 999 (2012) 34.

47 Amine Khodja I & Boulebd H, *Mol Divers*, 25 (2021) 279.

48 Milenković D, Đorović J, Jeremić S, Dimitrić Marković J M, Avdović E H & Marković Z, *J Chem*, 2017 (2017) 1.

49 Najafi M, Najafi M & Najafi H, *J Theor Comp Chem,* 12 (2013) 1250116.

50 Biela M, Kleinová A & Klein E, *Phytochem,* 200 (2022) 113254.

51 Deepha V, Praveena R & Sadasivam K, *J Mol Struc,* 1082 (2015) 131.

52 Jeremić S, Radenković S, Filipović M, Antić M, Amić A & Marković Z, *J Mol Graph Model*, 72 (2017) 240.

53 The Cambridge Crystallographic Data Centre. The Cambridge Structural Database (CSD). Https://Www.Ccdc.Cam.Ac.Uk/Structures/.

54 Marković Z, Tošović J, Milenković D & Marković S, *Comp Theor Chem*, 1077 (2016) 11.

55 Rimarčík J, Lukeš V, Klein E & Ilčin M, *J Mol Struct Theochem*, 952 (2010) 25.

56 Klein E, Rimar J & Lukeš V, *Acta Chim Slovaca,* (2009).

57 Shin M H, Moon Y J, Seo J E, Lee Y, Kim K H & Chung J H, *Free Radic Biol Med*, 44 (2008) 635.

58 Higgins P, Dawson J, Lees K R, McArthur K, Quinn T J & Walters M R, *Cardio Ther*, 30 (2012) 217.

59 Boulebd H, *J Biomol Struc Dyn*, 40 (2022) 10373.

60 Santi M D, Paulino Zunini M, Vera B, Bouzidi C, Dumontet V, Abin-Carriquiry A, Grougnet R & Ortega M G, *Eur J Med Chem*, 143 (2018) 577.

61 Ghallab D S, Shawky E, Metwally A M, Celik I, Ibrahim R S & Mohyeldin M M, *RSC Adv,* 12 (2022) 2843.

62 Cao H, Pauff J M & Hille R, *J Nat Prod*, 77 (2014)1693.

63 RCSB Protein Data Bank (RCSB PDB). Https://Www.Rcsb.Org/.

64 Auto-Dock Tools 1.5.7 Https://Autodock.Scripps.Edu/.

65 BIOVIA Discovery Studio.Https://Www.3ds.Com/Products/Biovia.

66 Bui Thanh T, Phuong T T, Thu H N, Mai P T, Hong K D T & Thi T N, *J Res Pharm*, 27 (2023) 2452.

67 ADMETlab. ADMET Prediction Webserver.Http://Admet.Scbdd.Com/Home/Index/.